Supplementary Information

Comparison of photoactivatable crosslinkers for in-gel immunoassays

Kristine Y. Tan, Surbhi Desai, Erum Raja, Chris Etienne, Brian Webb, and Amy E. Herr

Supporting Note 1: Synthesis of Diazirine Methacrylamide
Actual IUPAC name: N-(3-(3-(3-methyl-3H-diazirin-3-yl)propanamido)propyl)methacrylamide

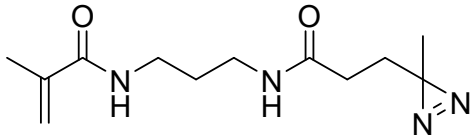

Diazirine Methacrylamide

Chemical Formula: $C_{12}H_{20}N_4O_2$
Molecular Weight: 252.32

Materials: NHS-diazirine (26167), Triethylamine (25108) and Dimethylformamide (20673) were purchased from Thermo Fisher Scientific. N-(3-Aminopropyl)methacrylamide hydrochloride (21200) was purchased from Polysciences. All commercially purchased materials were used without further purification unless stated otherwise. Bruker 400MHz Spectrometer was used for NMR analysis.
Procedure: A 250 mL, round bottom flask was equipped with a magnetic stir bar and charged with N-(3-Aminopropyl)methacrylamide hydrochloride (29.2 mmol, 1.0 eq.), DMF (80 mL) and triethylamine (32.2 mmol, 1.1 eq.) under N_2 atmosphere. NHS-diazirine (29.2 mmol, 1.0 eq) was added and reaction was stirred for 18-24 hours under N_2 at ambient temperature. Solids were removed by filtration and the filtrate was concentrated using a rotary evaporator. The concentrate was dissolved in dichloromethane (200 mL), washed with H_2O (2 × 100 mL), brine (2 × 100 mL) and dried over $MgSO_4$. The solvent was evaporated and the crude product was triturated using heptane (100 mL). Solids were filtered and dried in a vacuum oven overnight at 50 °C giving a white solid in 85% yield (99% purity via quantitative ^{1}H NMR using an internal standard (DIB, Diiodobenzene)).

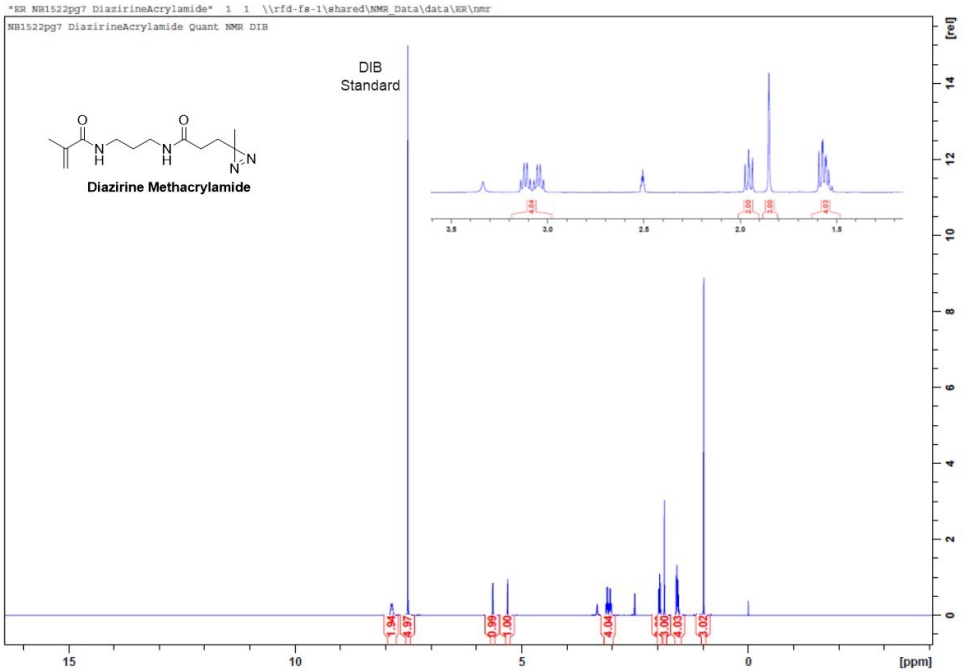

Fig. S1: ^{1}H NMR (DMSO-d6, 400 MHz): 7.8 (m, 2H), 5.7 (s, 1H), 5.3 (s, 1H), 3.15 (q, *J* = 4 Hz, 2H), 3.05 (q, *J* = 4 Hz, 2H), 1.95 (t, *J* = 4 Hz, 2H), 1.85 (s, 3H), 1.55 (m, 4H), 1.00 (s, 3H).

Figure S2 Probing additional targets (β-tubulin SFPQ) from single-cell lysate

We performed analysis of additional targets: β –tubulin (50 kDa) and SFPQ (95 kDa). (SFPQ has a reported molecular mass of 76 kDa, however based on the manufacturer's product information page, and previously reported western blot analysis from single-cell and bulk cell lysate[1–6], we hypothesize detection of a higher molecular mass species of ~95 kDa). β–tubulin and SFPQ both migrated ~1.4× farther in the DZMA gels than in BPMA gels. The mean electrophoretic mobility (μ) for β–tubulin was 0.0056 ± 0.0003 $mm^2/V{\cdot}s$ (n = 650 cells across 3 devices) in DZMA gels and 0.0041 ± 0.0002 $mm^2/V{\cdot}s$ (n = 729 cells across 3 devices) in BPMA gels. The mean electrophoretic mobility of SFPQ was 0.0024 ± 0.0002 $mm^2/V{\cdot}s$ (n = 76 cells across 2 devices) in DZMA gels and 0.0017 ± 0.0002 $mm^2/V{\cdot}s$ (n = 211 cells across 2 devices) in BPMA gels ($p < 0.01$; Mann-Whitney U Test). AUC of β–tubulin in DZMA gels was only ~28.4% of the β–tubulin AUC in BPMA gels. SNR of β–tubulin in DZMA gels was 37.6% of the SNR in BPMA gels ($p < 0.01$; Mann-Whitney U Test). For SFPQ, the AUC of SFPQ in DZMA was 42.9% of the AUC of SFPQ in BPMA gels. Furthermore, SNR of SFPQ peaks was 35.9% of the SFPQ SNR in BPMA gels ($p < 0.01$; Mann-Whitney U Test).

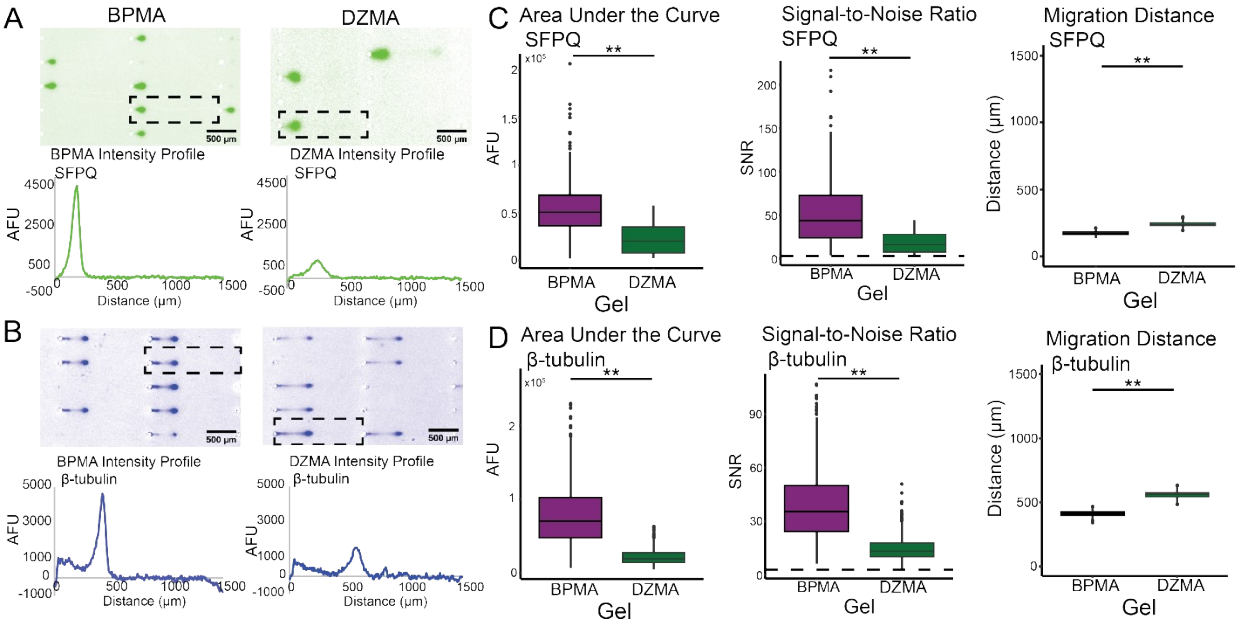

Fig. S2 Probing additional targets in DZMA hydrogels for single-cell immunoblotting to detect β-tubulin and SFPQ from MDA-MB-231 breast cancer cells. (A) Representative false-color fluorescence micrographs and intensity plots as examples of β-tubulin (50 kDa) and (B) SFPQ (Ab detects 95 kDa target according to product specification sheet, but actual predicted MW is 76 kDa) electromigration in each gel condition. Analysis of protein area under the curve (AUC) signal, SNR, and peak migration distance for (C) β-tubulin (50 kDa) and (D) SFPQ following immunoprobing of BPMA gels (purple) and DZMA gels (green). The AUC and SNR is much higher in BPMA gels indicating higher protein capture efficiency. Analysis of peak migration distance for β-tubulin and SFPQ indicate faster protein migration in the diazirine methacrylamide gels. N = 2-3 replicate devices per gel condition, ** $p < 0.01$; Mann-Whitney U Test."

Figure S3 Hydrogel swelling ratios in water and 70% IPA

Polyacrylamide precursor was prepared with 12 mM DZMA, 3 mM BPMA, or blank DMSO vehicle control. 1 mm thick gels were fabricated by pipetting polyacrylamide precursor solution between a clean glass plate and a ¼ of a standard microscope glass slide (18.75 × 25 cm), separated by gel casting spacers (C.B.S. Scientific GelWrap, 1 mm thickness) and polymerized for 1 hour. Gels were released from glass to create free-standing 1mm-thick hydrogels. To dose with UV, immediately after fabrication, gels were placed on a glass slide and exposed to collimated UV light under a mercury arc lamp (365 nm, at ~18.0 mW/cm^2; Optical Associates, Inc.) for 100 s to activate protein capture molecules. Gels were then placed back in MilliQ water to wash overnight (12-18 hours) to remove any salts from the gel. After washing, gels were placed in a 70°C oven until completely dehydrated (~4-6 h). Dehydrated gels were weighed on a scale (Mettler Toledo ME204E) to obtain the gel "dry weight". Gels were rehydrated by incubating in either MilliQ H_2O or 70% isopropyl alcohol. After 24 h of incubation, swollen gels were weighed again for the "swollen" weight. The swelling ratio (Q) was calculated as $Q = \frac{Weight_{swollen}}{Weight_{dry}}$.

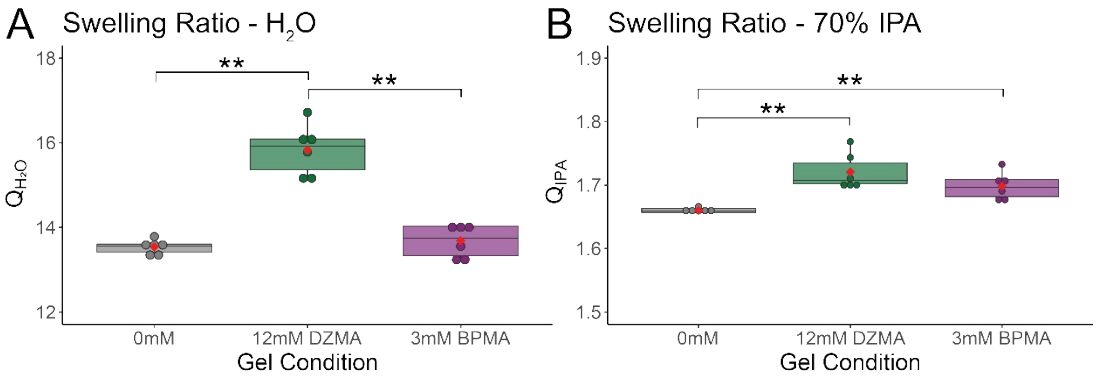

Fig. S3 Swelling ratios (Q) of 0 mM, 12mM DZMA hydrogels and 3 mM BPMA hydrogels in a (A) polar solvent, water and (B) nonpolar solvent 70% IPA. (A) 12 mM DZMA gels had significantly higher swelling ratio in water compared to both 3 mM BPMA and the 0 mM negative control. (B) Both 12 mM DZMA and 3 mM BPMA had significantly higher swelling ratios than the 0 mM negative control, but there was no significant difference between 12 mM DZMA and 3 mM BPMA gels. ** $p < 0.01$; Kruskal-Wallis with Holm multiple pairwise correction

Figure S4 Area under the curve (AUC) and signal-to-noise ratios (SNR) purified protein native separations

Purified Ova was labelled in-house using the described protocol in the DyLight 633 Antibody Labeling Kit, resulting in a degree-of-labelling of 0.28 fluorophores per molecule of protein. Labelled Ova was diluted to 2 µM concentration in 1× PBS. Gels for purified protein native microscale separations were polymerized on a silanized glass slide using wafers microfabricated with SU-8 3050 to have 100 µm diameter "posts" to form microwells that were ~60 µm in height. To run purified protein separations, 250 µL of protein solution was pipetted on the top of gels with 100 µm diameter microwells and 1 mm separation lane. The gel was incubated in protein solution for 90 seconds (>3τ diffusion timescale for protein to partition into the microwell but not the hydrogel). After incubation, the slide was transferred to the electrophoresis chamber and 17 mL of room-temperature non-denaturing run buffer (1× Tris-Glycine) was poured into the chamber and an electric field (E = 40 $V \cdot cm^{-1}$) was immediately applied to inject and separate proteins for 27 seconds in the PA gel abutting the microwell. After separation, proteins were immobilized in the gel matrix via a 45-second exposure to UV light (Lightningcure LC5, Hamamatsu) which activated the BPMA or DZMA functional group (incorporated during gel fabrication) to cross-link proteins to the gel matrix[7]. The UV light guide was held ~25 cm above the gel for all replicates. A fluorescence microarray scanner (Genepix 4300A, Molecular Devices) equipped with 4-laser lines (λ = 488, 532, 594, 635 nm) acquired fluorescence readout.

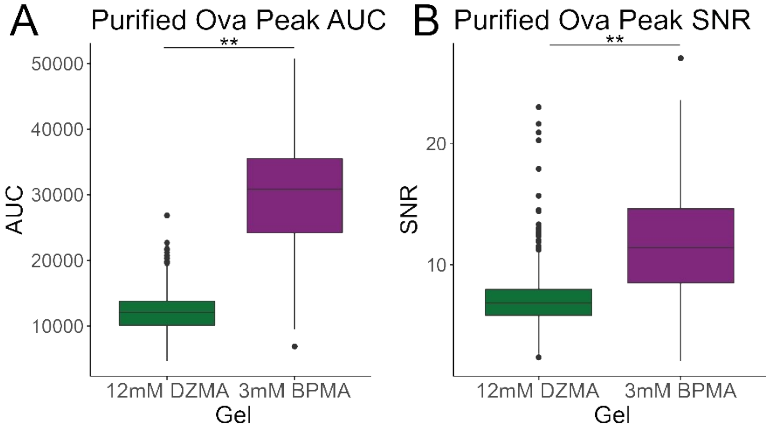

Fig. S4 AUC and SNR analysis of purified labelled ovalbumin after native microscale separations using 1× Tris-glycine run buffer. Both AUC and SNR are much higher in BPMA gels indicating higher protein capture efficiency even in non-denaturing conditions. N = 3 devices per gel condition, ** $p < 0.01$; Mann-Whitney U Test.

References

(1) Tan, K. Y.; Herr, A. E. Ferguson Analysis of Protein Electromigration during Single-Cell Electrophoresis in an Open Microfluidic Device. *Analyst* **2020**, *145* (10), 3732–3741. https://doi.org/10.1039/c9an02553g.

(2) Huang-Fu, N.; Cheng, J. S.; Wang, Y.; Li, Z. W.; Wang, S. H. Neat1 Regulates Oxidized Low-Density Lipoprotein-Induced Inflammation and Lipid Uptakein Macrophages via Paraspeckle Formation. *Mol. Med. Rep.* **2018**, *17* (2), 3092–3098. https://doi.org/10.3892/mmr.2017.8211.

(3) Cai, Y.; Wee, S. Y. K.; Chen, J.; Teo, B. H. D.; Ng, Y. L. C.; Leong, K. P.; Lu, J. Broad Susceptibility of Nucleolar Proteins and Autoantigens to Complement C1 Protease Degradation. *J. Immunol.* **2017**, *199* (12), 3981–3990. https://doi.org/10.4049/jimmunol.1700728.

(4) Nalvarte, I.; Schwend, T.; Gustafsson, J. Å. Proteomics Analysis of the Estrogen Receptor α Receptosome. *Mol. Cell. Proteomics* **2010**, *9* (7), 1411–1422. https://doi.org/10.1074/mcp.M900457-MCP200.

(5) Bottini, S.; Hamouda-Tekaya, N.; Mategot, R.; Zaragosi, L. E.; Audebert, S.; Pisano, S.; Grandjean, V.; Mauduit, C.; Benahmed, M.; Barbry, P.; et al. Post-Transcriptional Gene Silencing Mediated by MicroRNAs Is Controlled by Nucleoplasmic Sfpq. *Nat. Commun.* **2017**, *8* (1), 1–16. https://doi.org/10.1038/s41467-017-01126-x.

(6) Snijders, A. P.; Hautbergue, G. M.; Bloom, A.; Williamsom, J. C.; Minshull, T. C.; Phillips, H. L.; Mihaylov, S. R.; Gjerde, D. T.; Hornby, D. P.; Wilson, S. A.; et al. Arginine Methylation and Citrullination of Splicing Factor Proline- and Glutamine-Rich (SFPQ/PSF) Regulates Its Association with MRNA. *RNA* **2015**, *21* (3), 347–359. https://doi.org/10.1261/rna.045138.114.

(7) Kang, C.-C.; Yamauchi, K. A.; Vlassakis, J.; Sinkala, E.; Duncombe, T. A.; Herr, A. E. Single Cell–Resolution Western Blotting. *Nat. Protoc.* **2016**, *11* (8), 1508–1530. https://doi.org/10.1038/nprot.2016.089.